Intense reddish orange light emission and energy transfer of Eu^{3+} doped $NaGd(PO_3)_4$ for light emitting diodes LEDs application

Saoussen Hammami[a,], Nassira Chniba Boudjada[b] and Adel Megriche[a]

[a] *Université de Tunis El Manar, Faculté des Sciences de Tunis, UR11ES18 Unité de recherche de Chimie Minérale Appliquée. Campus Universitaire Farhat Hached, 2092 Manar 1. Tunis. Tunisie.*
[b] *Institut Néel, B.P. 166, 38042 Grenoble Cedex 9, France.*

(Received: 04 November 2017, accepted: 04 June 2018)

Abstract: A new alkali metal-rare earth polyphosphates $NaGd_{(1-x)}Eu_x(PO_3)_4$ (x= 0, 0.05, 0.10, 0.15) were prepared by solid state reaction. The obtained powders are identified by X-ray diffraction, Raman and Infrared spectroscopies. These polyphosphates crystallize in the monoclinic system with P $2_1/n$ space group and with cell parameters a= 7.174(1)Å, b= 13.033(2)Å, c= 9.781(1)Å, β= 90.65(2)°, V= 914.47(20)Å^3 and Z= 4. The structure of $NaGd(PO_3)_4$ is both $(PO_4)^{3-}$ zig-zag chains and an infinite chains formed by the alternate connection of GdO_8 polyhedra and LiO_4 tetrahedra. The compound has good thermal stability to 920°C. Magnetic susceptibilities of single crystals were measured in the temperature range of 5-300 K. The compounds were paramagnetic, and obeyed the Curie-Weiss law in the entire temperature interval, without magnetic phase transitions. Optical properties of the Eu^{3+} doped $NaGd(PO_3)_4$ were investigated under λ_{ex}= 394 nm and λ_{em}= 591 nm at 300K. The excitation spectra have revealed from 200 to 350 nm the presence of Gd^{3+} 4f-5d interconfiguration transitions, Gd^{3+}–O^{2-} and Eu^{3+}–O^{2-} charge transfer states (CTS) in addition to intraconfiguration transitions of Gd^{3+} ions. Eu^{3+} doped phosphors can emit intense reddish orange light. The strongest two at 590 and 613 nm can be attributed to the transitions from excited state $^5D_0$ to ground states $^7F_1$ and $^7F_2$, respectively.

Key words: NGP polyphosphates; Infrared spectroscopy; magnetic properties; Optical materials; Raman spectroscopy.

INTRODUCTION

Condensed alkali metal-rare earth polyphosphates with the general formula $M^IRE^{III}(PO_3)_4$ (where M^I = alkali metal and RE^{III}= rare earth ions) exhibit various structures [1-3]. They were characterized by high stability under normal conditions of temperature and humidity, and an almost isotropic thermal expansion with high chemical stability and high micro hardness [4-5]. Condensed polyphosphate can be employed in lasers [6], photo catalysts [7], fiber optics [8], sensors [9], and photoluminescent devices [10], etc. Currently, a great attention was focused on the spectroscopic characteristics of the Eu^{3+} ion in varied inorganic compounds [11, 12]. Particularly Eu^{3+} doped-phosphates are constantly the object of extensive structural and spectroscopic investigations. Some researchers synthesized rare earth ions doped LGP and investigated the luminescence properties of these phosphors. *Zhong et al.* prepared Ce^{3+} doped $MGd(PO_3)_4$ (M=Li,Na,K,Cs) powder samples and investigated the luminescence properties of these phosphors under X-ray irradiation [13]. *Han et al.* introduced Eu^{3+} into LGP and studied the luminescence properties [14]. The results of Han and co-workers show that Eu^{3+} doped LGP can emit intense red light under the excitation of vacuum ultraviolet (VUV) light. Thus, it is a promising red phosphor for mercury-free lamps and plasma display panel (PDP). However, the luminescence properties of Eu^{3+} in $NaGd(PO_3)_4$(NGP) excited with NUV lights have not been reported. This is very important for its applications in white light-emitting diodes.

* Corresponding author, e-mail address : adel.megriche@fst.utm.tn

This work describes the synthesis of $NaGd_{(1-x)}Eu_x(PO_3)_4$ polyphosphate, doped with different percentages of europium (5, 10 and 15%). The structural study of all obtained compounds is carried out with XRD diffraction. The infrared and Raman spectroscopies, magnetic and thermal analyses were recorded at room temperature. Moreover, the optical study through excitation and emission of Eu^{3+}ions spectra was also undertaken.

EXPERIMENTAL

The condensed phosphates $NaGd_{(1-x)}Eu_x(PO_3)_4$ (where x= 0, 0.05, 0,10 and 0.15) were synthesized by solid state reaction. A mixture of the following reagents: Na_2CO_3, Gd_2O_3, Eu_2O_3 and $NH_4H_2PO_4$ was prepared with the molar ratio (2.1:1:8) of Na:Gd:P respectively. First, the raw materials were grounding in an agate mortar for one hour at least to homogenize the solid phase and improve the inter-atomic diffusion. Second, the mixture was introduced into the oven and submitted to the following thermal program. The first level at 430°C to eliminate H_2O, NH_3 and CO_2, the second one, at 730°C to get $NaGd_{(1-x)}Eu_x(PO_3)_4$ pure phase. Then, the obtained products were cooled with the rate of 2°C/min to ensure a better crystallinity. Finally, the synthesized polyphosphates were washed with boiling water and nitric acid solution (1mol/L) to eliminate the residual raw materials from the final product.

Samples were characterized using a INEL XRG 3000 (D5000T) diffractometer with monochromatic Cu K_α radiation. The diffraction pattern was recorded under 300K over the angular range 10-90° (2Θ). The luminescence spectra were performed under ambient atmosphere via Xenius (the fluorescence Genius) spectrophotometer, at 591nm and 394nm for excitation and emission respectively. The infrared spectra were recorded in the range of 400-1500 cm^{-1} with a Thermo SCIENTIFIC NICOLET N10 MX. Raman analysis was carried out at room temperature, with 514.5 nm radiation from an argon ion laser as the excitation beam. A microscope allowed a selection of high optical quality region in the crystalline sample. Thermal stability of Eu^{3+} doped LGP was measured with differential thermal analysis SETARAM TAG 16 operating from room temperature up to 1000°C with heating rate of 5°C min^{-1}. Magnetic measurements were carried out using Quantum Design MPMSXL magnetometer with detection SQUID (at institute NEEL France).

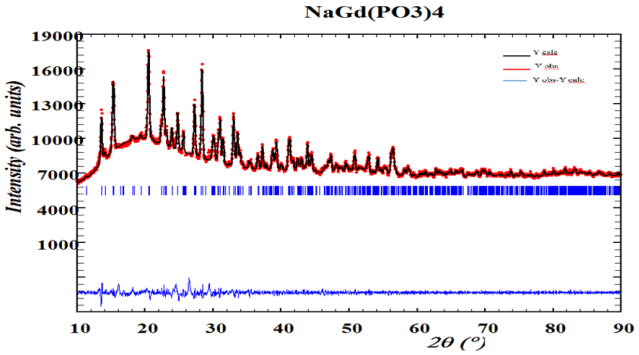

Fig 1: The Rietveld analysis of X-ray diffraction patterns for $NaGd(PO_3)_4$

RESULTAS AND DISCUSSION

1. Structural description

$NaGd_{(1-x)}Eu_x(PO_3)_4$ (where x= 0, 0.05, 0.10 and 0.15) sample prepared at high temperatures under 730°C would show colorless, transparent and parallelepiped-shaped. The morphology of obtaining polyphosphates crystals is shown in Fig 1. The sample prepared by solid state-reactions is stable in air and its crystallized into a monoclinic system, the XRD patterns of sodium gadolinium polyphosphates were indexed using Fullprof [15], from which the Bragg diffraction positions was confirms the crystal structure. The samples were of single-phase purity because no extra peak that corresponds to secondary phases or impurity was observed [16]. The samples were of single-phase purity because no extra peak that corresponds to secondary phases or impurity was observed. The $NaGd(PO_3)_4$ polyphosphate is isostructural with $CsGd(PO_3)_4$[17] and $CsEu(PO_3)_4$ [18]. It

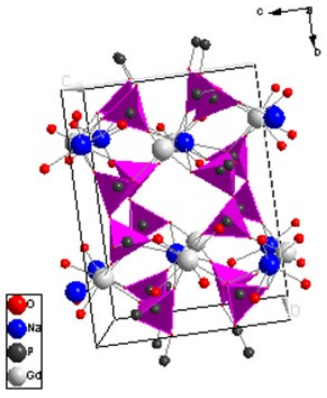

Fig 2: The structural arrangement of the unit cell of $NaGd(PO_3)_4$ in (100) plane.

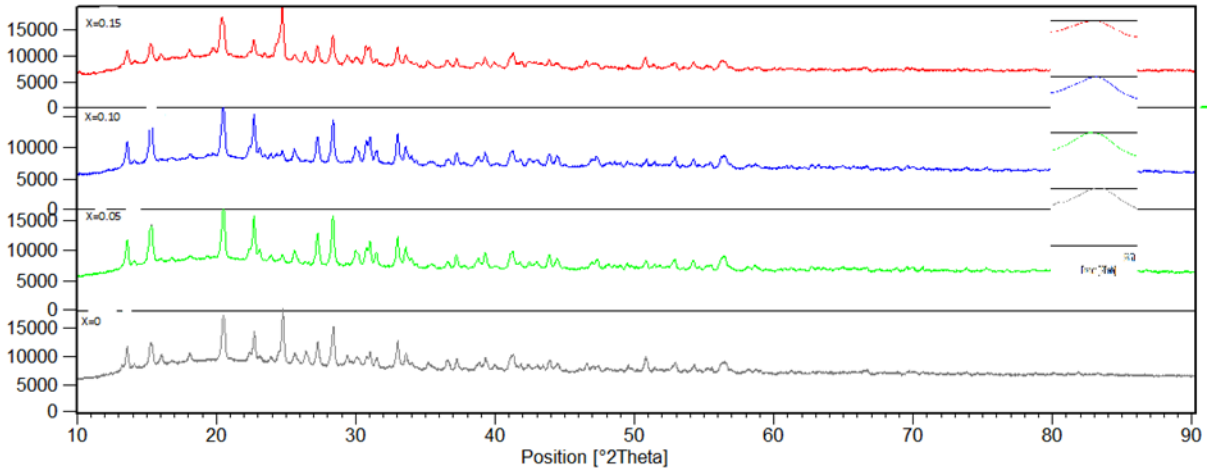

Fig 3: XRD patterns of samples $NaGd_{(1-x)}Eu_x(PO_3)_4$ (where x= 0, 0.05, 0.10 and 0.15)

crystallizes in the monoclinic system with P 21/n space group and with cell parameters a= 7.174(1) Å, b= 13.033(2)Å, c= 9.781(1)Å, β= 90.65(2)°, V= 914.47(20)Å^3 and Z= 4. The crystal structure of the title compound is described as an infinite three-dimensional (3D) framework (Fig. 2). Neighboring PO_4 tetrahedra are connected by bridging oxygen atom to form infinite double spiral chains. These polyphosphate chains are consisted by period of eight PO_4 tetrahedra (Fig. 2). These chains are joined to each other by GdO_8 and NaO_{11} polyhedra. The gadolunium (Gd^{3+}) and sodium (Na^+) ions are located inside infinite tunnels along the [0 11] direction.

Fig 3 shows the XRD patterns of samples with the different Eu^{3+}content. All the patterns are same at first sight. However, if we magnify these patterns locally it can be seen that there is slight difference in the position of diffraction peaks. The insets show the magnified part of the XRD patterns. It is clearly observed that from in doped LGP to the most doped one, in the process of the increment of Eu^{3+} content, the main diffraction peaks of samples gradually move to lower angles. These phenomena can be explained by Bragg's equation "2d sinΘ= λ" (where λ is the wavelength of the employed X-rays, Θ is the Bragg diffraction angle and d is the interplanar distance of corresponding diffraction peaks) that predicts that a theta-shifting to lower angles is due to the increase of the interplanar distance d, when Gd^{3+} is replaced Eu^{3+}, the ionic radius increases $R(Gd^{3+}_8)$= 0.1053 nm and $R(Eu^{3+}_8)$= 0.1066 [19].

2. Spectroscopic analysis

2.1. IR spectra

The rough interpretation of the spectra was made on the basis of characteristic vibration bands of $(O\text{-}P\text{-}O)^-$ group and POP bridge. A comparison with IR spectra of similar polyphosphate materials was used to assign tentatively the IR features [20-23].

The spectrum range pertinent to the present compound is 1400-400 cm^{-1}. Substantially, a large number of band were observed in this range due to the presence of four crystallographically different PO_4 tetrahedra as shown in Fig 4. In IR spectrum, the structure of this condensed polyphosphate based on an infinite chain of PO_4 tetrahedra bounded by a bridging.

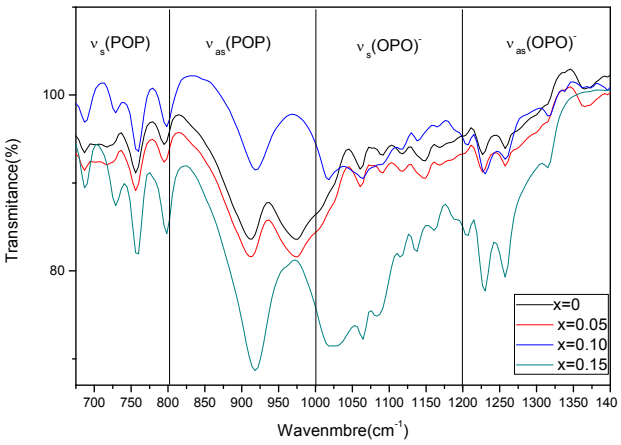

Fig 4: IR spectra of $NaGd_{(1-x)}Eu_x(PO_3)_4$ (x=0, 0.05, 0.10 and 0.15).

Tab I: Attributions of main IR bands (cm^{-1}) of $NaGd_{(1-x)}Eu_x(PO_3)_4$ (x= 0, 0.05, 0.10 and 0.15) samples.

Assignement	x=0	x=0.05	x= 0.10	x=0.15
υ_{as} OPO	1257 1137	1241 1127	1250 1149	1251 1149
υ_{s} OPO	1089	1089	1089	1089
υ_{as} POP	1014 944	1014 944	1014 947	1014 945
υ_{s} POP	689 736 761 818	689 736 758 818	689 736 761 818	689 736 765 818

Oxygen is confirmed by the absence of bands between 750 and 1000 cm^{-1}. Weak bands in the 1179-1060 cm^{-1} range are due to the symmetric vibrations (υ_s) of $(O\text{-}P\text{-}O)^-$ stretching in the PO_2 group. Sharp peaks present at 797, 758, 727, and 685 cm^{-1} are assigned to the symmetric vibrations (υ_s) of P-O-P. Band assignments for the vibrational modes of the $(PO_3)_4^{4-}$ phosphoric anions are presented in Table I.

2.2. Raman spectra

The Raman spectrum of $NaGd_{(1-x)}Eu_x(PO_3)_4$ (where x= 0, 0.05, 0.10 and 0.15) powder are showed in Fig 5. The line number is in almost agreement with that of previous IR bands [1]. The symmetric stretching vibrations υ_s (P–O–P) and υ_s $(O\text{-}P\text{-}O)^-$ in chain polyphosphate appear, respectively, in the range close to 700 and 1187 cm^{-1} as strong Raman line. The asymmetric vibration modes υ_{as}(P–O–P) and $\upsilon_{as}(O\text{-}P\text{-}O)^-$ are located, respectively, between 900-1143cm^{-1} and 1258-1300 cm^{-1} as fine Raman line. The bending vibration of $(O\text{-}P\text{-}O)^-$ and P–O–P appear between 607 and 250cm^{-1}.

3. DTA (Differential Thermal Analysis)

The thermal stability of lithium polyphosphate is investigated using DTA. The curves of the Eu: $NaGd(PO_3)_4$ crystal are given in Fig 6. It is clearly observed that the curves present the same shape (evolution). Indeed, a single sharp endothermic peak is observed between 900 and 1000°C for all samples, which exhibits the characteristics of a first-order phase transition. This signal can be attributed to the decomposition of polyphosphates to $GdPO_4$ [24]. Hence, it can be concluded that all samples are monophasic.

4. Magnetic study

The magnetic susceptibility versus temperature of $NaGd(PO_3)_4$, $NaGd_{0.95}Eu_{0.05}(PO_3)_4$, $NaGd_{0.90}Eu_{0.10}(PO_3)_4$ and $NaGd_{0.85}Eu_{0.15}(PO_3)_4$ are shown in Fig 7. This figure proves that all for rare-earth polyphosphate compounds exhibit a paramagnetic response. The non-doped NGP is the most paramagnetic one; this is explained by their structural stability of its structure. Indeed, the addition of europium in the host disturbs samples crystallinity.

The theoretical magnetic moment in units of Bohr magnetons (γ_B) of a free ion Ln^{3+} is determined by the following formula [25]:

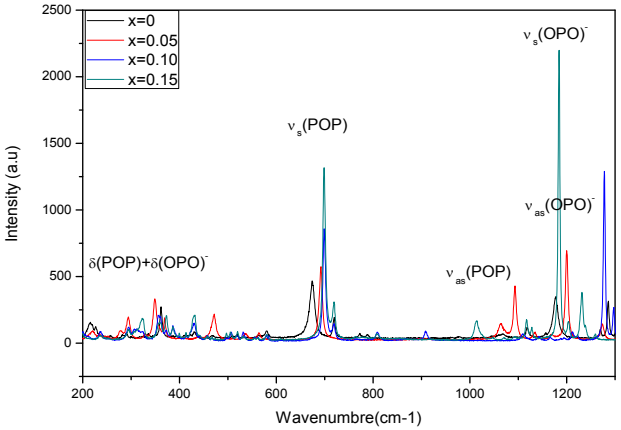

Fig 5: Raman spectra of $NaGd(PO_3)_4$ (x=0, 0.05, 0.10 and 0.15) at 300 K.

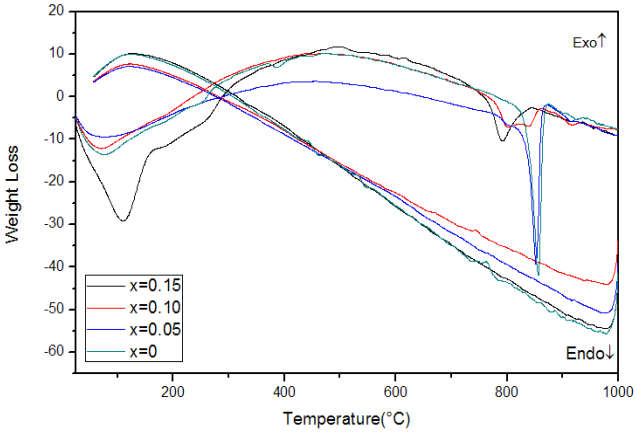

Fig 6: DTA of $NaGd_{(1-x)}Eu_x(PO_3)_4$ (x=0, 0.05, 0.10 and0.15).

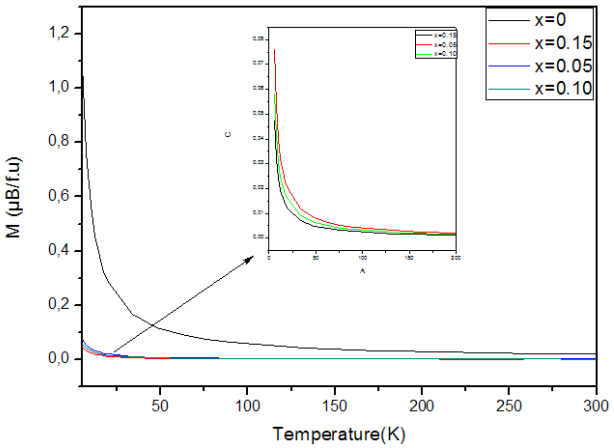

Fig 7: The magnetic susceptibility (χ) as function of temperature of $NaGd_{(1-x)}Eu_x(PO_3)_4$ (x=0, 0.05, 0.10 and 0.15).

$$\mu_{eff} = g_J\sqrt{J(J+1)}$$

Where g_J is the Lande factor and J is the total angular moment.

$$g=1+[J(J+1)-L(L+1)+S(S+1)]/2J(J+1)$$

The temperature dependence of the inverse of susceptibility χ^{-1} in high temperatures is given by the following formula:

$$\frac{1}{\chi} = \frac{(T-\theta_p)}{C}$$

Where Θ_P is the Weiss temperature and C is the Curie constant given by:

$$C \approx \frac{\mu_0 N \mu_{eff}^2}{3K_B}$$

Where N is the number of carriers of magnetic moment, μ_0 is the vacuum permeability, K_B is the Boltzmann constant, μ_B is the Bohr magnetron and μ_{eff} is effective moment of carriers. Samples structure consists of one magnetic species (i), possessing each a magnetic moment μ_{eff} (i), the magnetic susceptibility is given by the relation:

$$\chi = \mu_0 \frac{n_1\mu_{eff}^2(1) + n_2\mu_{eff}^2(2) + ... + n_i\mu_{eff}^2(i)}{3K_BT}$$

Curves of χ^{-1} (Fig 8) versus temperature allow deducing μ_{eff}^{exp} values, which are summarized in Table II. We can notice that the values of

Tab II: Values of C, μ_{eff}^{the} (μ_B), μ_{eff}^{exp} (μ_B) of $NaGd_{(1-x)}Eu_x(PO_3)_4$ (x=0, 0.05, 0.10 and 0.15) compounds.

	x=0	x=0.05	x=0.10	x=0.15
C ($\mu_B.KT^{-1}$)	3.053	2.78	2.72	1.63
μ_{eff}^{the} (μ_B)	7.94	7.543	7.146	6.49
μ_{eff}^{exp} (μ_B)	4.92	4.69	4.64	3.59

μ_{eff}^{the} decrease with the decrease of Gd percentage in the system, due to the important magnetic moment of Gd^{3+} ions ($7.94\mu_B$). The comparison between the theoretical and the experimental effective moment values, shows that former are higher than the latter. This result can be associated to the increase of disorder in the matrix (NGP). On the other side, when the temperature increases to more than 75K, it induces a thermal agitation and causes magnetic moments disorientation of atoms in Eu doped NGP polyphosphates. Consequently, a decrease of paramagnetism is clearly observed (Fig 7).

5. LUMINESCENCE PROPERTIES

5.1. Emission

Fig 9 displays the room temperature emission spectra of NGP:Eu^{3+} powders synthesized by solid

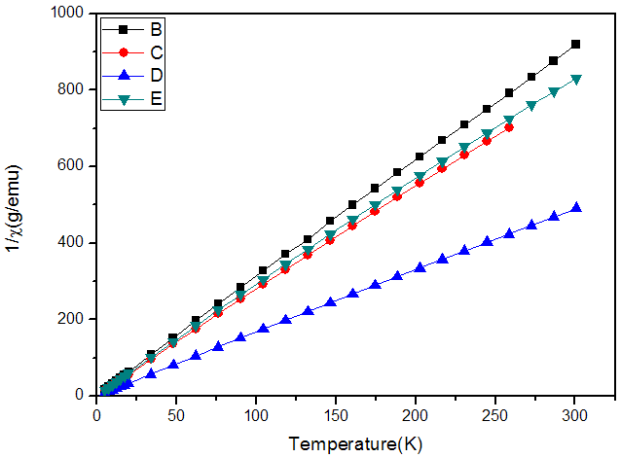

Fig 8: The inverse magnetic susceptibility (1/χ) measurements as a function temperature of $NaGd_{(1-x)}Eu_x(PO_3)_4$ (x=0, 0.05, 0.10 and0.15).

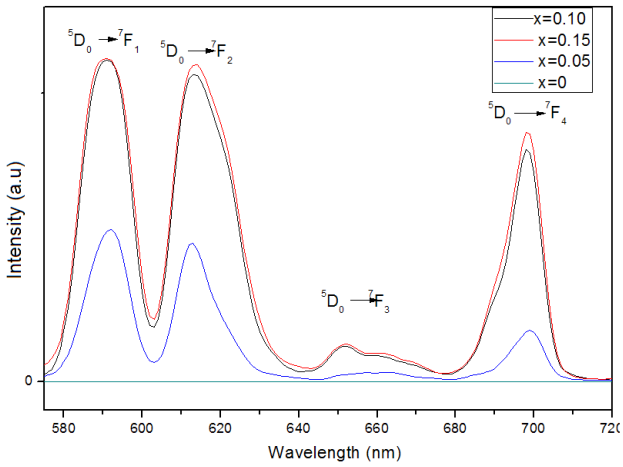

Fig 9: Emission spectra with λ_{ex}=394 nm of $NaGd_{(1-x)}Eu_x(PO_3)_4$ (x=0, 0.05, 0.10 and 0.15) at 300 K.

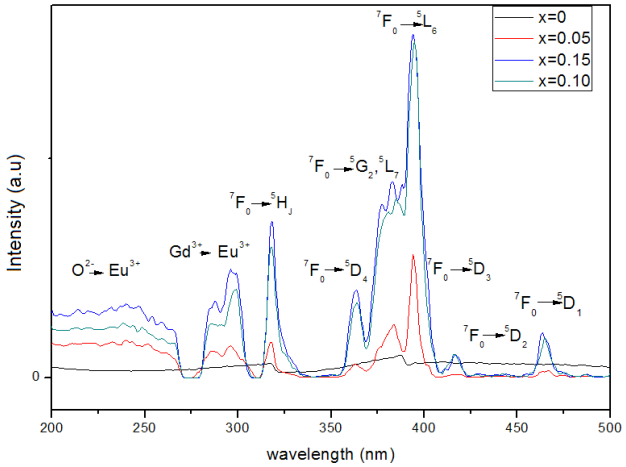

Fig 10: Excitation spectra with λ_{em}=591 nm of $NaGd_{(1-x)}Eu_x(PO_3)_4$ (x=0, 0.05, 0.10 and 0.15) at 300 K.

state reaction. Upon VUV excitation at 394 nm. These spectra present the same shapes, with bands intensity proportional to Eu^{3+} active ion concentration. However, we notice that the undoped $NaGd(PO_3)_4$ polyphosphate does not emit light. These spectra are constituted of several peaks in the 575-720 nm wavelength range. The assignment of the various emission to transitions involving the Eu^{3+}, from $^5D_0$ level as emitting level to the receiver ones ^7F_J (J= 0, 1,2,3 and 4) are indicated in Table III. The relative intensities of the most intense transitions $^5D_0 \rightarrow ^7F_1$, $^7F_2$ are strongly influenced by the nature of the host and the crystalline environment [26]. Therefore, the dominance of magnetic dipole (MD) transition $^5D_0 \rightarrow ^7F_1$ of Eu^{3+} means that Eu^{3+} occupies a site in the crystal lattice with inversion symmetry. However, in the case of absence of symmetry inversion in the site of Eu^{3+}, the main emission would be the electric dipole (ED) transition $^5D_0 \rightarrow ^7F_2$ [27]. NGP: Eu^{3+} showed that orange emission transition ($^5D_0 \rightarrow ^7F_1$) is slightly dominated. We concluded that Eu^{3+} occupies a site in the crystal lattice with symmetry inversion.

Tab III: Emission attribution of Eu^{3+} doped $NaGd(PO_3)_4$.

Wavelength (nm)	Attribution
577-602	$^5D_0 \rightarrow ^7F_1$
604-634	$^5D_0 \rightarrow ^7F_1$
643-669	$^5D_0 \rightarrow ^7F_1$
680-709	$^5D_0 \rightarrow ^7F_1$

5.2. Excitation

Fig 10 shows the excitation spectra of all compounds monitoring the emission at 591 nm. It is observed that all the excitation spectra are composed of one broad band in 200-250 nm range. Thus can be attributed to the charge transfer band (CTB), resulting from the transfer of an electron from the orbital $2p^6$ of the ligand O^{2-} to the empty state of the configuration $[Xe]4f^6$ of the Eu^{3+} ion (Eu^{3+}-O^{2-} transition).

Tab IV: Excitation bands attribution of Eu^{3+} doped $NaGd(PO_3)_4$.

Wavelength (nm)	Attribution
287	$^7F_0 \rightarrow ^5I_6$
294	$^7F_0 \rightarrow ^5F_4$
297	$^7F_0 \rightarrow ^5F_2$
318	$^7F_0 \rightarrow ^5H_6$
321	$^7F_0 \rightarrow ^5H_4$
328	$^7F_0 \rightarrow ^5H_7$
363	$^7F_0 \rightarrow ^5D_4$
376	$^7F_1 \rightarrow ^5D_4$
373-390	$^7F_0 \rightarrow ^5G_{J(2,4)}$
394	$^7F_0 \rightarrow ^5L_6$
405	$^7F_1 \rightarrow ^5L_6$
416	$^7F_0 \rightarrow ^5D_3$
464	$^7F_0 \rightarrow ^5D_2$
526	$^7F_0 \rightarrow ^5D_1$

At low frequencies, several groups of narrow bands in the spectral region 271-310 nm are clearly observed and assigned to $^8S_{7/2}\rightarrow{}^6H_J$, $^8S_{7/2}\rightarrow{}^6G_J$, $^8S_{7/2}\rightarrow{}^6D_J$, $^8S_{7/2}\rightarrow{}^6I_J$, and $^8S_{7/2}\rightarrow{}^6P_J$ transitions of the Gd^{3+} ion. $LiYF_4:Gd^{3+}$ crystal is used as reference to identify excitation bands, which describe the basis of the detailed energy level scheme proposed for the trivalent gadolinium [28].

Excitation bands in the 271-310 nm range confirmed energy transfer between the two rare earths, which occurs from Gd^{3+} to Eu^{3+} in the matrix. Above 310 nm excitation bands can be attributed to the intra-configurational 4f-4f transitions of Eu^{3+} in the host lattice: $^7F_0\rightarrow{}^5H_J$ at 317 nm, $^7F_0\rightarrow{}^5D_4$ at 363 nm, $^7F_0\rightarrow{}^5G_2$, $^5L_7$ at 382 nm, $^7F_0\rightarrow{}^5L_6$ at 393 nm, $^7F_0\rightarrow{}^5D_3$ at 416 nm, $^7F_0\rightarrow{}^5D_2$ at 464 nm and $^7F_0\rightarrow{}^5D_1$ at 500 nm [29-30]. All these assignments and wavelengths are given in Table IV.

Particularly, some broadened excitation lines overlap together and form a strong excitation band from 370 to 408 nm with a full width at half maximum (FWHM) of 18 nm. The perfect matching of this excitation band with the emission wavelength of NUV InGaN-based LED chips makes these phosphors be used in white LEDs conveniently [31].

CONCLUSION

We successfully grew a condensed phosphates single crystal of 5, 10 and 15% Eu^{3+}-doped $NaGd(PO_3)_4$ with very good crystallinity using solid state reaction at 730°C. XRD patterns proved that the obtained samples crystallize in a monoclinic single phase with P 2_1/n space group and with cell parameters a= 7.174(1) Å, b= 13.033(2)Å, c= 9.781(1)Å, β= 90.65(2)°, V= 914.47(20)$Å^3$ and Z= 4. The phosphate structure can be described as a long chain polyphosphate organization containing an alternating zigzag chains $(PO_3)_n$ and (Gd^{3+},Na^+) cations along the b direction. NGP: Eu^{3+} has good thermal stability under 900°C. The magnetic susceptibility carried out on single crystals revealed that the title compounds were paramagnetic between 5 and 300 K. Eu^{3+} doped NGP can be effectively excited by NUV light from 370 to 408 nm and emit intense reddish orange light ($^5D_0\rightarrow{}^7F_1$). Therefore, the phosphor NGP:Eu^{3+} may be considered as a suitable candidate for light emitting diodes LEDs application.

REFERENCES

[1] S. Sebai, S. Hammami, A. Megriche, D. Zambon, R. Mahiou, *J. Optical Materials*. **2016**, 62, 578-583.

[2] A. Durif, Crystal Chemistry of Condensed Phosphates, *Plenum Press*, New York, **1995**.

[3] N. Ben Hassen, M. Ferhi, K. Horchani-Naifer, M. Férid, *J. Materials Research Bulletin*. **2015**, 63, 99-104.

[4] M. Ferhi, K. Horchani-Naifer, M. Ferid, *J. Optical Materials*. **2011, 34,** 12-18.

[5] I. Parreu, R. Sole, J. Massons, F. Diaz, M. Aguilo, *J. Cryst. Growth Des*. **2007**, 7(3), 557.

[6] J.H. Campbell, T.I. Suratwala, *J. Non-Cryst. Solids*. **2000**, 263-264, 318-341.

[7] D. Jing, L. Guo, *J. Phys. Chem*. **2007**, C 111, 13437-13441.

[8] Y.C. Yan, A.J. Faber, H. De Waal, P.G. Kik, A. Polman, *J. Appl. Phys. Lett*. **1997**, 71, 2922-2924.

[9] D. Kozlova, V. Sokolova, M. Zhong, E. Zhang, J. Yang, W. Li, Y. Yang, J. Buer, A. Westendorf, M. Epple, H. Yan, Virol. Sin. **2014**, 29, 33-39.

[10] Z. Wang, W. Duan, X. Cui, C. Liang, R. Zheng, W. Wei, *J. Mater. Chem*. **2014**, C 2, 4012-4018.

[11] J. Hao, S.A. Studenikin, M. Cocivera, J. Lumin. **2001**, 93, 313.

[12] M. Ferhi, K. Horchani-Naifer, M. Ferid, *J. Rare Earth*. **2009**, 27, 82.

[13] J.P. Zhong, H.B. Liang, Q.Su, J.Y. Zhou, I.V. Khodyuk, P. Dorenbos, *J. Opt.Mater*. **2009**, 32, 378-381.

[14] B. Han, H.B. Liang, H.Y.Ni, Q.Su, G.T.Yang, J.Y.Shi, G.B.Zhang, *J. Opt.Express*. **2009**, 17, 7138-7144.

[15] J. Rodriguez-Carvajal, FULLPROF version July **2006**, ILL (unpublished).

[16] S. Hammami, S. Sebai, D. Jegouso, V. Reita, N. C. Boudjada, A. Megriche, *J. Journal of Physical Chemistry & J Biophysics.* **2017**, 7, 1000255.

[17] H. Naïli, T. Mhiri, *J. Acta Crystallogr*. **2005**. E 61, i204-i207.

[18] J. Zhu, W.D. Cheng, H. Zhang, *J. Acta Crystallogr*. **2009**, E 65, i70.

[19] R.D. Shannon, J. Acta Cryst. **1976**. A32, 751-767.

[20] I. Szczygieł, L. Macalik, E. Radominska, T. Znamierowska, M. Maczka, P.Godlewska, J. Hanuza, *J. Opt. Mater*.**2007**, 29, 1192.

[21] W. Jungowska-Hornowska, L. Macalik, R. Lisiecki, P. Godlewska, A. Matraszek,I. Szczygieł, J. Hanuza, *J. Mater. Chem. Phys*. **2009**, 117, 262.

[22] J. Amami, M. Ferid, M. Trabelsi-Ayedi, *J. Mater. Res. Bull*. **2005**, 40, 2144.

[23] A. Jouini, M. Ferid, M. Trabelsi-Ayedi, *J. Mater. Res. Bull*. **2003**, 38, 437.

[24] H. Ettis, H. Naï¨lI, T. Mhiri, *J. Journal of Solid State Chemistry*. **2006**, 179 3107–3113.

[25] D. Petrov, B. Angelov, V. Lovchinov, *J. Journal of rare earths*.**2013**, 31, 485.

[26] D.C. Tuan, R. Olazcuaga, F. Guillen, A. Garcia, B. Moine and C. Fouassier, *J. J. Phys*. IV France. **2005**, 123, 259–263.
[27] M. Gaft, G.Panczer, R.Reisfeld, I.Shinno, B.Champagnon, G.Boulon, *J. Lumin*. **2000**, 87-89, 1032–1035.
[28] R. T. Wegh, H. Donker, A. Meijerink, R. J. Lamminmaki, and J. Holsa, *J. Phys. Rev*. **1997**, B 56, 13841.
[29] S. Hachani, B. Moine, A. El-akrmi, M. Ferid, *J. Opt Mater*, **2009**, 31, 678-684.
[30] M. Ferhi, K. Horchani-Naifer, M. Ferid, *J. Optical Materials*. **2011**, 34, 12–18.
[31] M. Abdelhedi K. Horchani-Naifer M. Dammak M. Ferid, *J. Materials Research Bulletin*, **2015**, 70, 303-308.

Figures

Fig 1: The Rietveld analysis of X-ray diffraction patterns for $NaGd(PO_3)_4$

Fig 2: The structural arrangement of the unit cell of $NaGd(PO_3)_4$ in (100) plane.

Fig 3: XRD patterns of samples $NaGd_{(1-x)}Eu_x(PO_3)_4$ (where x= 0, 0.05, 0.10 and 0.15)

Fig 4: IR spectra of $NaGd_{(1-x)}Eu_x(PO_3)_4$ (x=0, 0.05, 0.10 and 0.15).

Fig 5: Raman spectra of $NaGd(PO_3)_4$ (x=0, 0.05, 0.10 and 0.15) at 300 K.

Fig 6: DTA of $NaGd_{(1-x)}Eu_x(PO_3)_4$ (x=0, 0.05, 0.10 and0.15).

Fig 7: The magnetic susceptibility (χ) as function of temperature of $NaGd_{(1-x)}Eu_x(PO_3)_4$ (x=0, 0.05, 0.10 and 0.15).

Fig 8: The inverse magnetic susceptibility ($1/\chi$) measurements as a function temperature of $NaGd_{(1-x)}Eu_x(PO_3)_4$ (x=0, 0.05, 0.10 and0.15).

Fig 9: Emission spectra with λ_{ex}=394 nm of $NaGd_{(1-x)}Eu_x(PO_3)_4$ (x=0, 0.05, 0.10 and 0.15) at 300 K.

Fig 10: Excitation spectra with λ_{em}=591 nm of $NaGd_{(1-x)}Eu_x(PO_3)_4$ (x=0, 0.05, 0.10 and 0.15) at 300 K.

Table Captions:

Tab I: Attribtions of main IR bands (cm^{-1}) of $NaGd_{(1-x)}Eu_x(PO_3)_4$ (x= 0, 0.05, 0.10 and 0.15) samples.

Tab II: Values of C, μ_{eff}^{the} (μ_B), μ_{eff}^{exp} (μ_B) of $NaGd_{(1-x)}Eu_x(PO_3)_4$ (x=0, 0.05, 0.10 and 0.15) compounds.

Tab III: Emission attribution of Eu^{3+} doped $NaGd(PO_3)_4$.

Tab IV: Excitation bands attribution of Eu^{3+} doped $NaGd(PO_3)_4$.